

Numerical Simulation of Solidification in Additive Manufacturing of Ti Alloy by Multi-Phase Field Method

Yusuke Shimono^{1*}, Mototeru Oba¹, Sukeharu Nomoto¹, Yuichiro Koizumi², and Akihiko Chiba²

1 ITOCHU Techno-Solutions Corporation, 3-2-5, Kasumigaseki, Chiyoda-ku, Tokyo 100-6080 Japan

2 Institute of Materials Research, Tohoku University, 2-2-1, Katahira, Aoba-ku, Sendai 980-8577 Japan

*Corresponding author

Email: yuusuke.shimono@ctc-g.co.jp

Abstract

The multi-phase field method (MPFM) coupled with the database of calculation of phase diagrams (CALPHAD) is a powerful tool for simulation of solidification microstructure evolution in engineering casting conditions. MPFM equations have been introduced assuming quasi-equilibrium at the interface. However, few attempts have been made adopting MPFM for solidification in additive manufacturing (AM) conditions because the process is considered to be in a strongly non-equilibrium condition. In other words, the classical solidification theory based on the local equilibrium assumption was not considered to be applicable to this process. However, some researchers have reported experimental observations of the columnar-to-equiaxed transition in the solidification of AM. These suggest MPFM can be adopted for solidification simulation of the AM process. We tackled the issue of applicability of MPFM for solidification simulation in AM of Ti alloys. It was confirmed that solidification simulation using MPFM can provide observation of the columnar-to-equiaxed transition and establish a solidification map for the AM process conditions.

Introduction

Simulation methods according to the classical solidification theory based on the local equilibrium assumption enable prediction of the grain microstructure and morphological evolution. Among the models available for microstructure evolution, Monte Carlo simulations, cellular automata, and the phase field method are the most widely used simulation methods [1]. The multi-phase field method (MPFM) coupled with the database of calculation of phase diagrams (CALPHAD) has been successfully applied for solidification microstructure evolution in standard casting conditions.

In the classical solidification theory, the solidification map is also a useful tool for predicting solidification microstructure. The solidification map shows the columnar-to-equiaxed transition (CET) with functions of the temperature gradient G and growth rate R . Using the solidification map, we can easily predict the relative grain size and morphology of the solidification microstructure [2].

Additive manufacturing (AM) is currently used for a wide range of processes from low-cost, consumer market to high-end direct metal systems. Electron beam melting (EBM) is a high-end AM method capable of producing complex parts. In the EBM process, the size of the melting pool is microscale and its temperature can reach several thousand degrees Celsius when the electron beam is applied to the metal. The cooling rate in EBM reaches several hundred thousand K/s and shows a large temperature gradient of about several hundred thousand K/m [3, 4]. This is considered to be a highly non-equilibrium process. The classical solidification theory based on the local equilibrium assumption was considered not to be applicable for the analysis of this process.

However, some recent works have reported experimental observations of CET in solidification of AM [5, 6]. CET is a phenomenon that can be explained by the classical solidification theory. This suggests MPFM could possibly be adopted for the solidification simulation of AM processes. MPFM based on the local equilibrium assumption is adapted to AM solidification in this study.

Many researchers currently consider the solidification map a useful item to predict a solidification microstructure during the AM processes and attempt to produce these maps for the solidification processes in AM by experiment [3, 5]. However, few studies so far have attempted to adopt numerical simulations for solidification simulation of the AM processes [4, 7].

We attempted to investigate the issue of applicability of MPFM coupled with the CALPHAD database for solidification simulation in the AM process of the Ti-6Al-4V alloy, widely used in the medical field, the aircraft industry, and the advanced aerospace industry due to its high specific strength and excellent corrosion resistance. We tackled determining the microstructure evolution of solidification for Ti-6Al-4V in the EBM processes. The solidification map was established with the microstructures obtained using various EBM conditions.

Multi-Phase Field Method

The multi-phase field method (MPFM) proposed by Steinbach approximately 20 years ago has been applied to many numerical simulation fields [8] and is expressed as shown below. The development of the phase field parameter ϕ_i of a phase i in a n multi-phase system is described by Equation (1).

$$\frac{\partial \phi_i}{\partial t} = \sum_{j=1}^n K_{ij} \left\{ \gamma_{ij} \left[\phi_j \nabla^2 \phi_j - \phi_i \nabla^2 \phi_i + \frac{\pi^2}{2\delta^2} (\phi_i - \phi_j) \right] + \frac{\pi}{\delta} \Delta G_{ij} \sqrt{\phi_i \phi_j} \right\} \quad (1)$$

K_{ij} is the interface mobility, γ_{ij} is the interface energy, δ is the interface thickness and ΔG_{ij} is the driving force for the transformation between the phases i and j . The driving force is obtained using the Gibbs free energy and chemical potential values estimated using the CALPHAD database.

Overall composition c^α for an N -components system is dependent on the following diffusion equation:

$$\frac{dc^\alpha}{dt} = \nabla \cdot \sum_{i=1}^n \left[\phi_i \sum_{i=1}^{N-1} {}^i D_{\alpha\beta}^N \nabla C_i^\beta \right] \quad (2)$$

Multi-phase diffusion for a component α is then given as the sum of the flux in the individual phases, calculated from the composition gradients and the diagonal terms ${}^i D_{\alpha\beta}^N$ of the diffusivity matrix. The diffusivity matrix values are obtained by the CALPHAD database and diffusion mobility database.

In particular, the CALPHAD database coupling method that uses the TQ-Interface of Thermo-Calc provides us a means to simulate the microstructure evolution of many engineering metal alloy processes [9]. For example, MICRESS® is a typical software tool for general commercial application [10]. In this study, we used MICRESS for MPFM solidification simulation. We used SSOL6 [11], which is the database for general alloys including Ti, Al, V, as the thermodynamic database and MOBTE [12], which is the specialized Ti-based database, as the diffusion mobility database.

Thermal analysis of EBM

The numerical simulations were performed according to the following steps:

- 1) Obtaining temperature profiles in the Ti-6Al-4V alloy powder bed at different electron beam powers and scan speeds.
- 2) Simulating solidification microstructure evolutions of Ti-6Al-4V alloy using MPFM for the temperature profiles obtained in step 1.
- 3) Establishment of solidification map using results of step 2.

To execute thermal profile simulation, we used a three-dimensional (3D) finite-element method (FEM) thermal model by implementing ABAQUS [13], as shown in Figure 1 (a). We performed thermal conduction analysis using a moving heat source model for EBM. In this model, heat transfer between the moving heat source plane (object *A*) and the surface of the powder bed (object *B*) is described by a heat transfer model, as shown in Figure 1 (b). Equation (3) gives the heat flux q between surfaces *A* and *B*.

$$q = k(\theta_A - \theta_B) \tag{3}$$

θ_A and θ_B are the temperatures *A* and *B* are at, respectively. k is the heat transfer coefficient. The heat flux of the moving heat source was assumed to depend on a Gaussian distribution according to Equation (4).

$$q_s(r) = \frac{q_{total}}{2\pi\sigma^2} \exp\left(-\frac{r^2}{2\sigma^2}\right) \tag{4}$$

where r is the polar coordinate radius, σ is the standard deviation of the radius of the heat flux distribution, and q_{total} is the overall heat flux of the moving heat source.

We assumed that the thermal conduction of the powder bed of the Ti alloy could be approximated as bulk metal conduction [14]. The bulk metal region was modeled as a part of a semi-infinite 1/4-elliptic cylinder, as shown in Figure 1 (a). Its horizontal length was 13.4 mm, vertical length was 6.7 mm, and longitudinal length was 32 mm. The thermal conductivity of the Ti-6Al-4V alloy as a function of temperature was determined by the Materials Properties Handbook [15] and ASM Handbook [16]. The initial uniform temperature of the metal region was 730 °C (1003 K) because of preheating. The size of σ is taken to be 0.255 mm, which was adjusted to be approximately the same experimental observation of the width of the melting pool [17]. Figure 1 (b) shows an image representing the thermal conduction simulation in this study. The translucent green disc represents the moving heat source and the rigid colored area is the bulk metal.

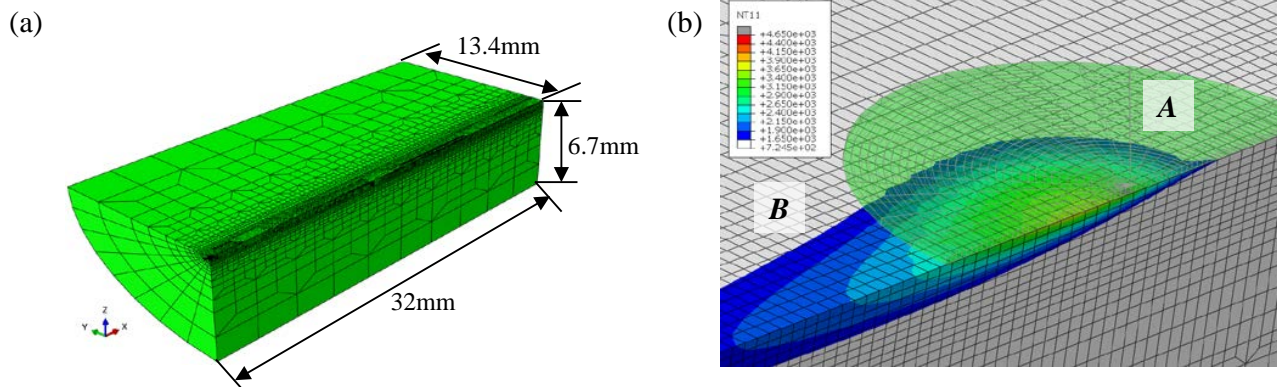


Figure 1. (a) Finite element model for a bulk metal; (b) a snapshot of thermal conduction simulation

In EBM processes, shapes of the melting pool are considered to be highly complex because of the Marangoni effect [18]. Therefore, it was still very difficult to conduct simulations accurately in three dimensions. In addition, it was necessary to predict the solidification microstructure transformation for various local temperature gradients and cooling rates for the establishment of the solidification map. In this study, we simulated only the thermal conductivity without taking the effect of fluid flow into account. Furthermore, in the solidification simulation, we simulated a two-dimensional (2D) solidification field on the plane perpendicular to the beam scan direction. This 2D solidification field was coupled with a one-dimensional (1D) temperature field perpendicular to the direction of the depth from the surface. The 1D temperature field was referred the 3D temperature field at a time of the FEM thermal conductive analysis. Figure 2 shows the procedure of setting the 1D temperature field.

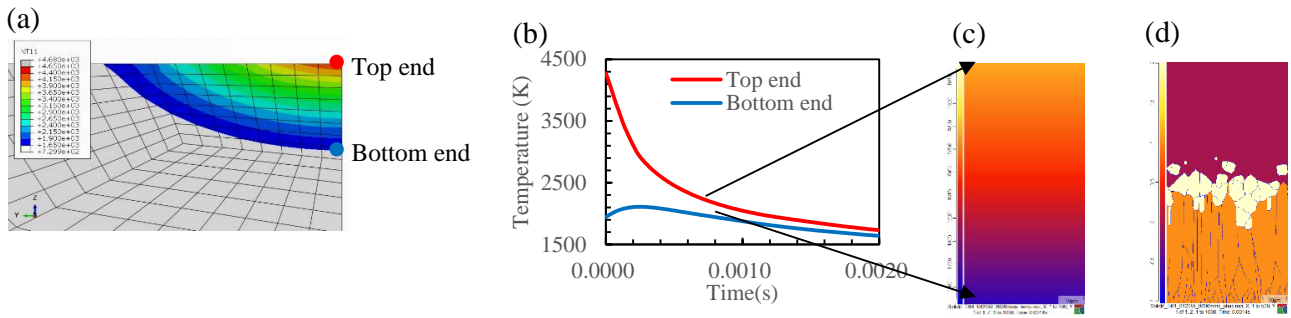


Figure 2. Procedure of setting 1D temperature field for MPFM solidification simulation: (a) the 3D FEM thermal conduction simulation, (b) 1D temperature profile transformed from the 3D FEM simulation in (a), (c) the 1D temperature field obtained using 1D temperature profiles in (b) for boundary conditions, (d) the MPFM solidification simulation coupled with the 1D temperature field in (c)

Calculation Conditions

One of the issues in this study was the simulation of CET varying with the temperature gradient and solidification rate. In this study, we used nucleation conditions for equiaxed grains as shown in Table 1. The seed density model is a type of nucleation model implemented in MICRESS [19]. This model is able to automatically select the density and radius of nuclei depending on the undercooling rate of the molten metal. Figure 3 shows the seed density distribution used in this study.

Table 1. Nucleation conditions of equiaxed grains

Condition	Value
Nucleation model	Seed density model
Maximum nucleation temperature (K)	1971
Time interval (s)	1×10^{-5}
Nucleation range	Liquid phase
Nuclei orientation	Random

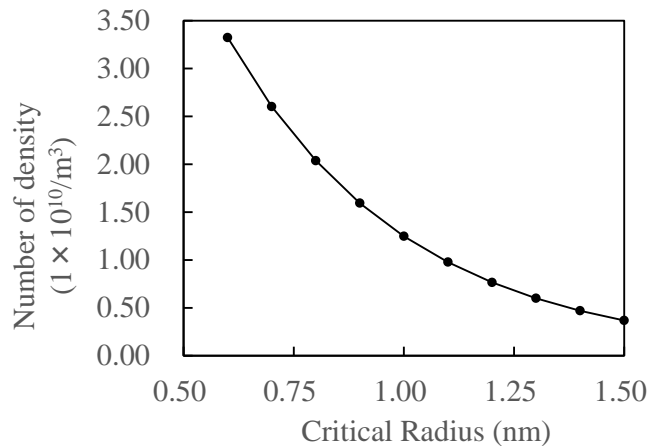


Figure 3. Seed density distribution in this study

Electron beam conditions used in this study are shown in Table 2. We considered four cases with different electron beam conditions to obtain thermal profiles and solidification simulations using these thermal profiles. The sizes of melting pools obtained from the determination of the thermal conduction are shown in Table 3.

Table 2. Electron beam conditions

Case #	Power (W)	Scan speed (m/s)	Line energy (J/m)
1	180	0.8	225
2	660	3.2	206
3	1280	6.4	200
4	420	0.8	525

Table 3. Melting pool sizes according to thermal conduction simulation

Case #	Width (μm)	Depth (μm)
1	340	50
2	440	60
3	460	50
4	500	140

Melting pool sizes were measured from the size of the region where the temperature was over the melting temperature of Ti-6Al-4V, 1650 °C (1923 K). Melting pool sizes for Case 4 were significantly larger than those for other cases. The regions of solidification simulation were set as shown in Table 4.

Table 4. Solidification simulation region sizes

	Width (μm)	Depth (μm)
Cases 1, 2, and 3	50	50
Case 4	50	100

Figure 4 shows the temperature profiles of these cases. The red lines denote the temperatures of the top end of the melting pools and the blue lines denote the temperature at a depth of 50 μm (Case 1, 2, and 3) or 100 μm (Case 4) for the melting pool, which represented the bottom of the solidification simulation region.

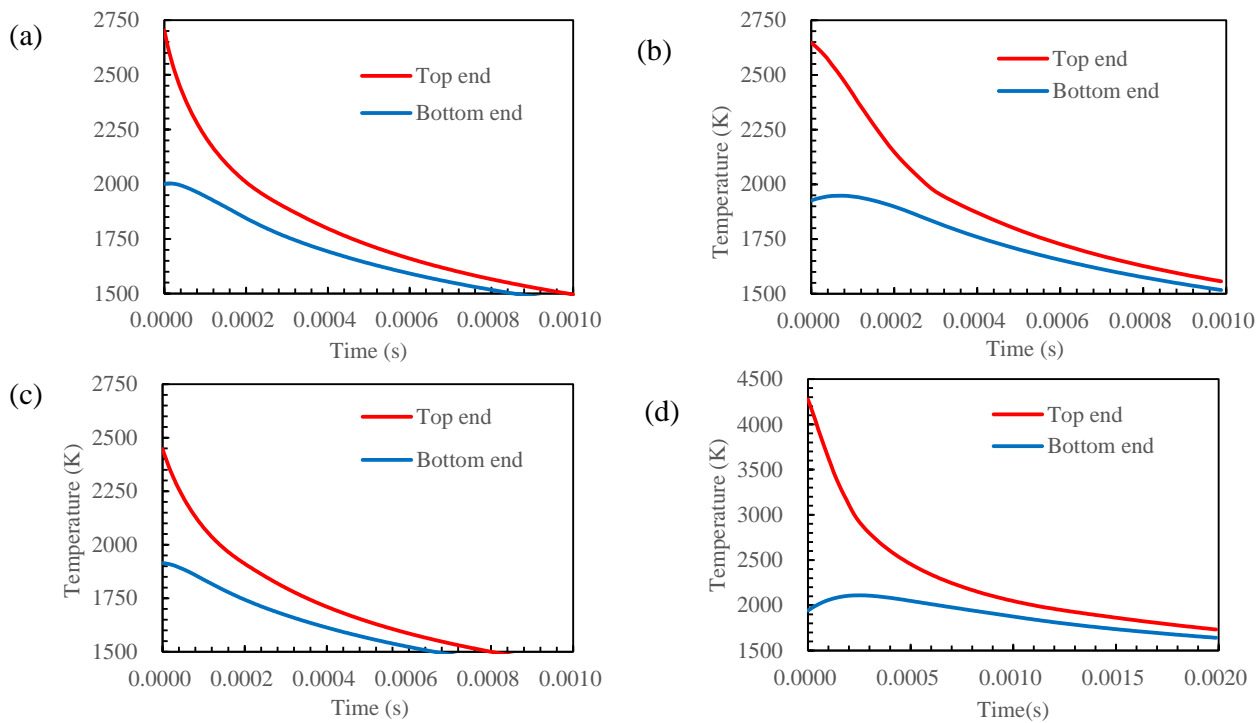


Figure 4. Thermal profiles obtained using FEM simulation
 (a) Case 1, (b) Case 2, (c) Case 3, and (d) Case 4

Table 5 shows the interface energy and interface mobility between liquid and β -Ti in this study. The interface energy was estimated by the extended Becker's model [20, 21].

Table 5. Interface energy and interface mobility

Interface energy (J/m ²) [20, 21]	Interface mobility (m ⁴ /Js)
0.8	1.5

Table 6 shows other parameters for the simulation region size. Case 1, 2, and 3 involved the same conditions, but Case 4 was different because the melting pool size was larger than in other cases. Initial phase distributions were set as liquid uniformly and temperatures were higher than the melting point (1650 °C). Nuclei of columnar grains were set to be generated at the bottom, which were set to be under the melting point with random crystal orientations.

Table 6. Geometry of simulation region for solidification

	Cases 1, 2, and 3	Case 4
Cell size	0.1 $\mu\text{m} \times 0.1 \mu\text{m}$	0.1 $\mu\text{m} \times 0.1 \mu\text{m}$
Number of cells	500 \times 500	500 \times 1000
Width of solidification field	50 μm	50 μm
Height of solidification field	50 μm	100 μm
Cell size of temperature field	10 μm	10 μm
Height of temperature field	50 μm	100 μm

Results and Discussion

The phase distributions for MPFM solidification simulation for Cases 1, 2, 3, and 4 are shown in Figure 5, 6, 7, and 8, respectively. It can be seen that columnar grains nucleate at the bottom and grow competitively at early times in all cases. After that, equiaxed grains nucleated in front of the growth direction of the columnar grains. By comparing equiaxed grain distributions for these cases, we can see that the grain size of Case 4 is larger than those of other cases. The number of and average radius of equiaxed grains in these cases are shown in Table 7. The grain number and size for Case 4 was confirmed to be evidently different from other cases according to the differences in the melting pool depth shown in Table 3. These CET tendencies in some beam conditions were confirmed by comparing experimental measurements [22].

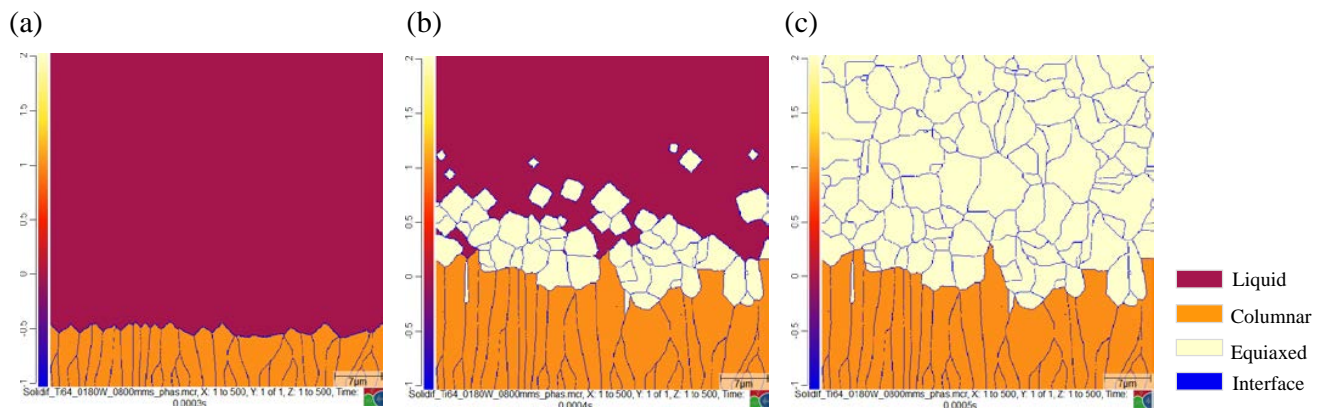


Figure 5. Phase distributions of Case 1 at (a) 0.0003 s, (b) 0.0004 s, and (c) 0.0005 s

(a) (b) (c)

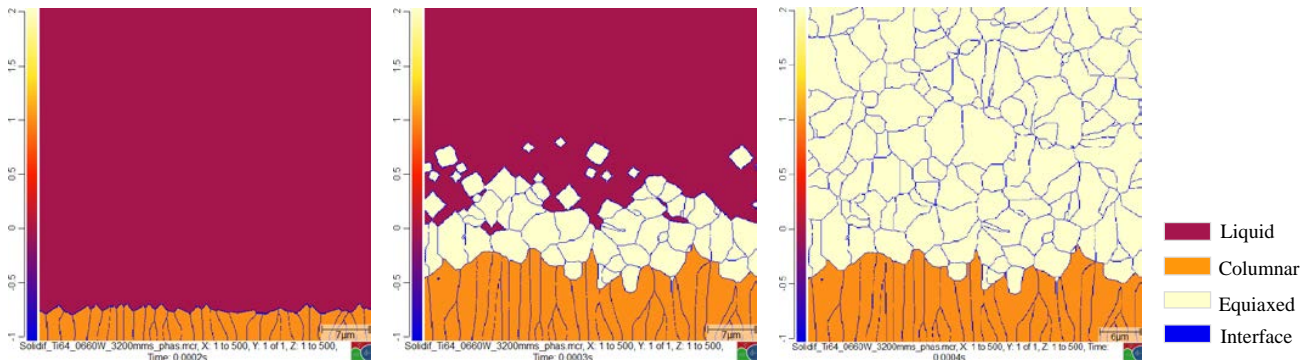


Figure 6. Phase distributions of Case 2 at (a) 0.0002 s, (b) 0.0003 s, and (c) 0.0004 s

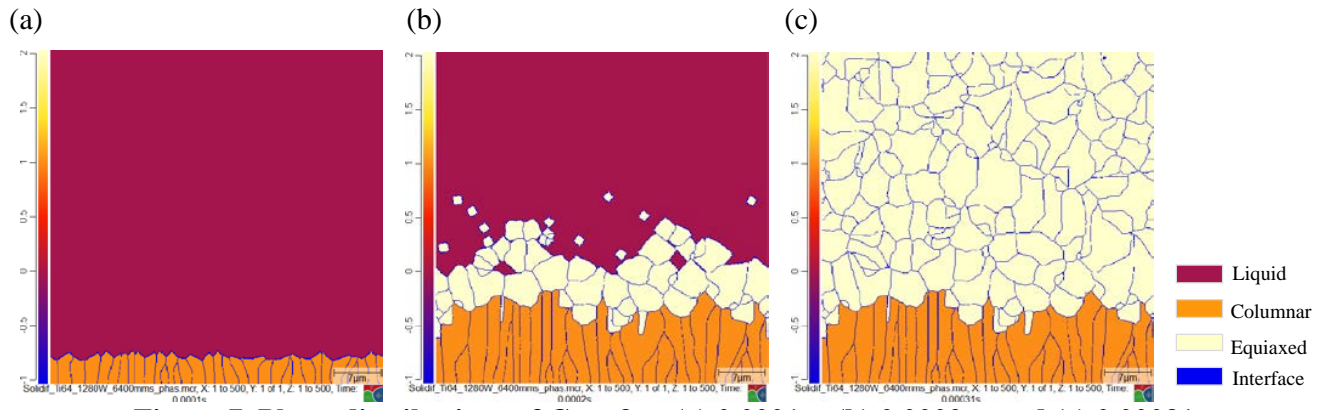


Figure 7. Phase distributions of Case 3 at (a) 0.0001 s, (b) 0.0002 s, and (c) 0.00031 s

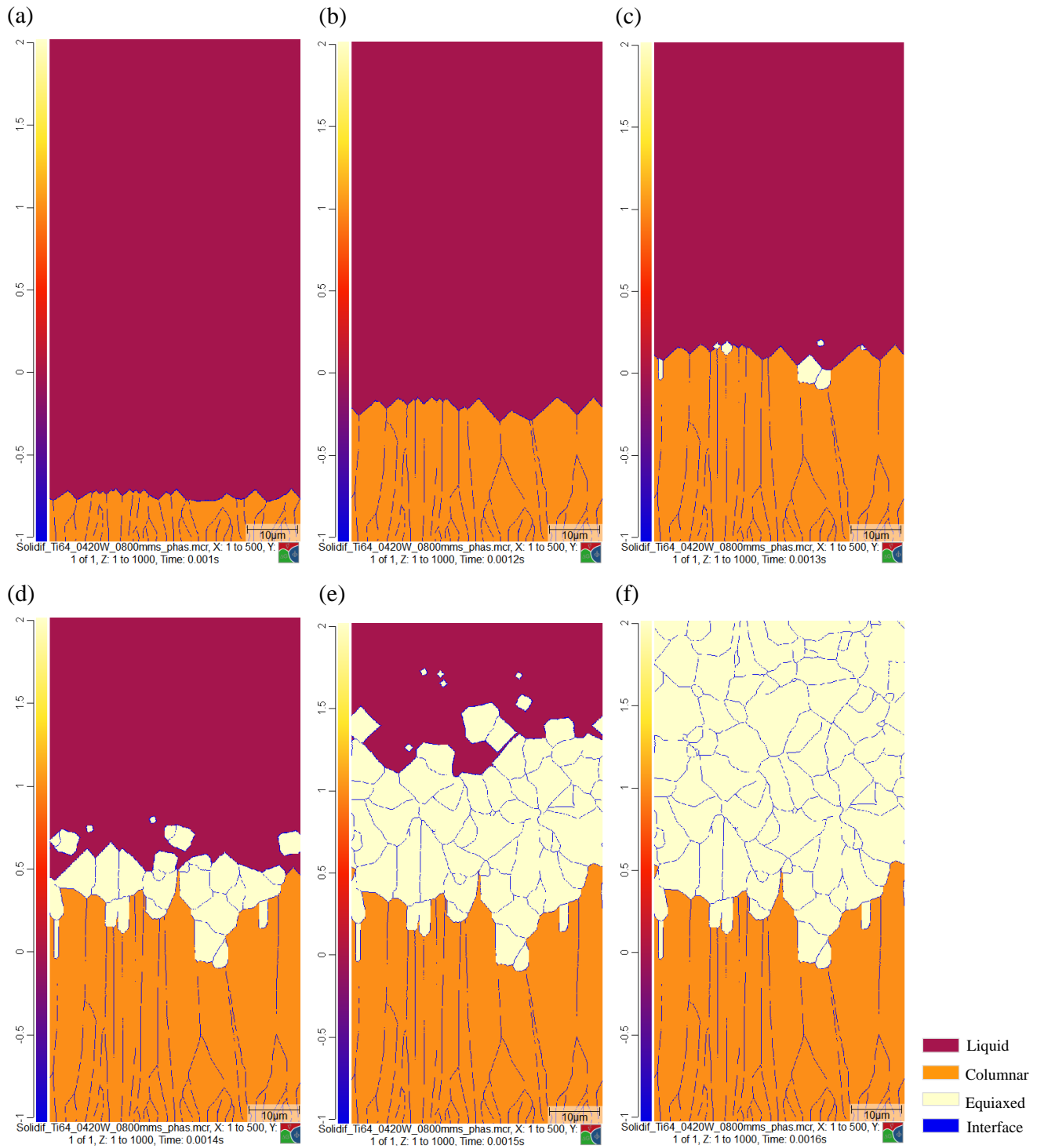


Figure 8. Phase distributions of Case 4 at (a) 0.001 s, (b) 0.0012 s, (c) 0.0013 s, (d) 0.0014 s, (e) 0.0015 s, and (f) 0.0016 s

Table 7. Number and average radius of equiaxed grain

Case #	Number of grains	Average grain radius (μm)
1	133	2.00
2	157	1.97
3	173	1.88
4	95	3.09

Using the results of the solidification simulation with MPFM, we plotted the temperature gradient (G) and solidification rate (R) at the solidification interface for a series of time-steps for Cases 1, 2, 3 and 4, as shown in Figure 9. The G and R values of columnar grain growth and equiaxed grain growth are plotted as blue and red symbols, respectively. Yellow plots show mixed grain growth points.

Figure 9 shows the columnar and equiaxed regions. It can be seen that these regions are separated by a transition region in all cases. Case 4 plots are placed far away from those of other cases, in the bottom left side. This means that the equiaxed grain size for Case 4 is coarser than in other cases. Therefore, a solidification map for Ti-6Al-4V alloy can now be constructed to predict the solidification morphology and the scale of the microstructure. Furthermore, these results confirm that this simulation method has the ability to produce a solidification map for the AM process.

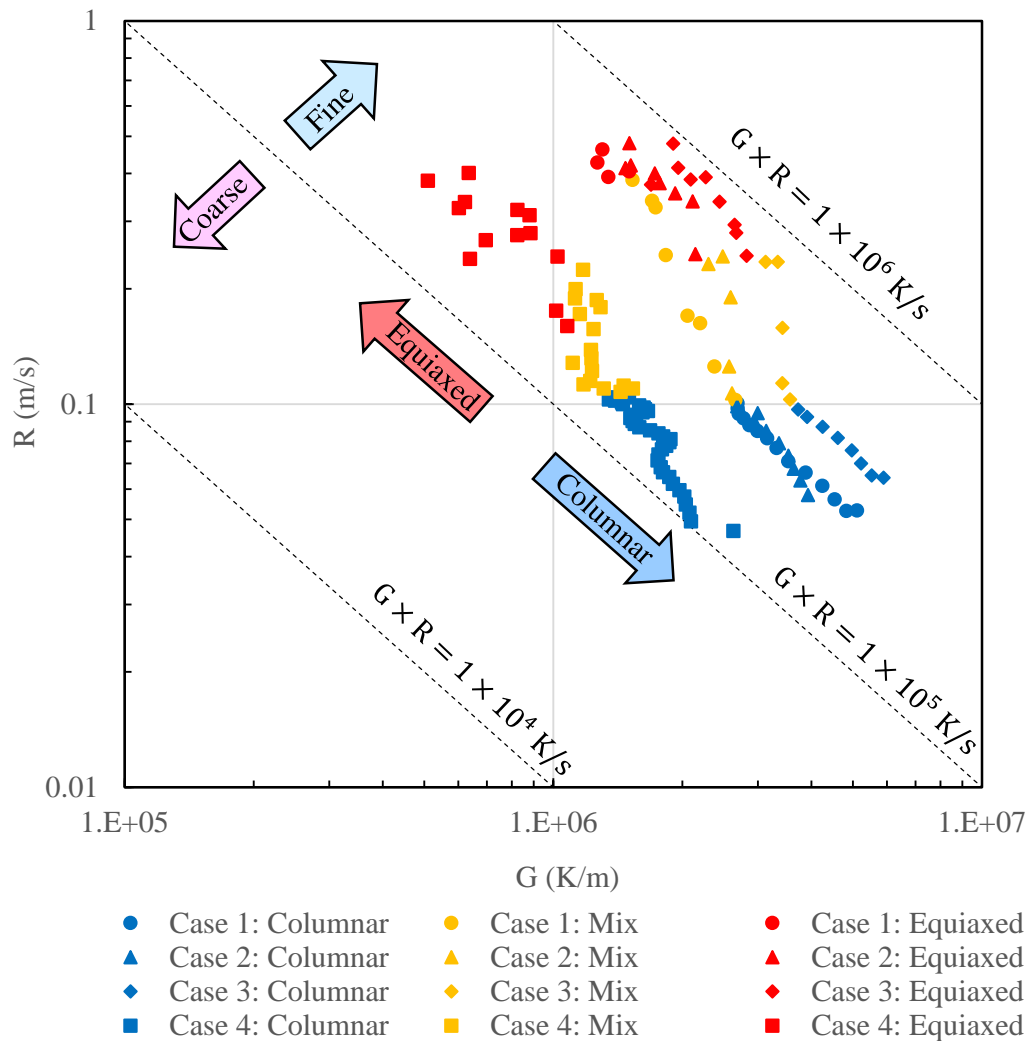


Figure 9. Solidification map of Ti-6Al-4V using solidification simulations of MPFM

Conclusion

We performed solidification simulation of Ti-6Al-4V in EBM processes using MPFM coupled with a CALPHAD database assuming local quasi-equilibrium. MPFM was also performed by coupling with a 1D temperature distribution obtained by FEM thermal conductivity analysis. We confirmed the CET results for several EBM conditions. In addition, we indicated the possibility of constructing a solidification map for AM

processes using the CET results. This numerical method offers significant potential for simulating the solidification microstructure evolution in AM processes.

References

- [1] N. Xiao, Y. Chen, D. Li, and Y. Li, "Progress in mesoscopic modeling of microstructure evolution in steels" *Sci. China Technol. Sci.* 55, 341, 2012.
- [2] P. Kobryn and S. Semiatin, "Microstructure and Texture Evolution during Solidification Processing of Ti-6Al-4V", *Journal of Materials Processing Technology*, 135, 330-339, 2003.
- [3] S.S. Al-Bermani, M. L. Blackmore, W. Zhang and I. Todd, "The Origin of Microstructural Diversity, Texture, and Mechanical Properties in Electron Beam Melted Ti-6Al-4V", *Metallurgical and materials transactions A*, 41A, 3422-3434, 2010.
- [4] X. Gong and K. Chou, "Phase-Field Modeling of Microstructure Evolution in Electron Beam Additive Manufacturing", *JOM*, 67, 5, 1176-1182, 2015.
- [5] Y. M. Ren, X. Lin, X. Fu, H. Tan, J. Chen and W.D. Huang, "Microstructure and deformation behavior of Ti-6Al-4V alloy by high-power laser solid forming", *Acta Materialia*, 132, 82-95, 2017.
- [6] C. Körner, H. Helmer, A. Bauereiß and R.F. Singer, "Tailoring the grain structure of IN718 during selective electron beam melting", *MATEC Web of Conferences 14*, 08001, 2014.
- [7] R. Martukanitz, P. Michaleris, T. Palmer, T. DebRoy, Z. K. Liu, R. Otis, T. W. Heo and L. Q. Chen, "Toward and integrated computational system for describing the additive manufacturing process for metallic materials", *Additive Manufacturing*, 1-4, 52-63, 2014.
- [8] J. Eiken, B. Boettger and I. Steinbach, "Multiphase-field approach for multicomponent alloys with extrapolation scheme for numerical application", *Phys. Rev. E*, 73 066122, 1-9, 2006.
- [9] Thermo-Calc Software AB, Software Development Kits:
<http://www.thermocalc.com/products-services/software/software-development-kits/>, 2017/6/26.
- [10] ACCESS e.V., MICRESS: <http://web.micress.de/>, 2017/6/26.
- [11] Thermo-Calc Software AB, SSOL6 SGTE Solutions Database version 6.0:
<http://www.thermocalc.com/products-services/databases/thermodynamic/>, 2017/6/26.
- [12] Thermo-Calc Software AB, MOBTTI Ti-alloys Mobility Database version 1.0:
<http://www.thermocalc.com/products-services/databases/mobility/>, 2017/6/26.
- [13] Dassault Systèmes K.K., Abaqus Unified FEA
: <http://www.3ds.com/products-services/simulia/products/abaqus/>, 2016/3/24.
- [14] S. Bontha, N. W. Klingbeil, P. A. Kobryn, H. L. Fraser, "Effects of process variables and size-scale on solidification microstructure in beam-based fabrication of bulky 3D structures", *Material Science and Engineering A*, 513-514, 311-318, 2009.
- [15] Materials Properties Handbook: Titanium Alloys, 1st ed., *ASM International*, 514-515, 1994.
- [16] ASM Handbook, Volume 15: Casting, *ASM International*, 468-481, 2008.
- [17] Unpublished research.
- [18] Y. Zhao, Y. Koizumi, K. Aoyagi, K. Yamanaka, and A. Chiba, "Modeling and Simulation of Electron Beam Additive Manufacturing for Biomedical Co-Cr-Mo Alloy", *Proceedings of the Visual-JW2016*, 3, 48-49, 2016.
- [19] S. Nomoto, S. Minamoto and K. Nakajima, "Numerical Simulation for Grain Refinement of Aluminum Alloy by Multi-phase-field Model Coupled with CALPHAD", *ISIJ International*, 49, 7, 1019-1023, 2009.
- [20] R. Becker, "Die Keimbildung bei der Ausscheidung in metallischen Mischkristallen", *Ann. Phys.*, 424, 128-140, 1938.
- [21] Thermo-Calc Software AB, Precipitation module (TC-PRISMA): [http://www.thermocalc.com/products-services/software/precipitation-module-\(tc-prisma\)/](http://www.thermocalc.com/products-services/software/precipitation-module-(tc-prisma)/), 2017/6/26.
- [22] J. Gockel and J. Beuth, "Understanding Ti-6Al-4V Microstructure Control in Additive Manufacturing via Process Map", *Solid Freeform Fabrication Proceedings*, 666-674, 2013